

# Broadband second-harmonic generation in $\text{Sr}_x\text{Ba}_{1-x}\text{Nb}_2\text{O}_6$ by spread spectrum phase matching with controllable domain gratings

Moshe Horowitz, Alexander Bekker, and Baruch Fischer

Department of Electrical Engineering, Advanced Optoelectronics Research Center, Technion-Israel Institute of Technology, Haifa 32000, Israel

(Received 23 November 1992; accepted for publication 17 February 1993)

We have demonstrated, for the first time to our knowledge, second-harmonic generation for a broad input wavelength range of 750–1064 nm in  $\text{Sr}_x\text{Ba}_{1-x}\text{Nb}_2\text{O}_6$  crystals, with a controllable spread spectrum of quasiphase matching. Second-harmonic conversion efficiencies of up to  $\sim 1\%$  were observed. This was done without any temperature or angular tuning of the crystal. The phase matching was obtained by inducing alternating ferroelectric domains in the crystal in real time, using a novel fixing process which is based on screening. The broadband capability of the conversion is allowed by a spread in the range of the domain widths.

The experimental demonstration of optical second-harmonic generation (SHG) in the early 60s (Ref. 1) was one of the basic landmarks in the early stages of nonlinear optics and lasers.<sup>2</sup> The recent years witnessed a renewed interest in the subject, mainly due to potential needs for efficient SHG with moderate light powers from compact sources, such as laser diodes. This motivation has led to the discovery of new nonlinear media, including organic crystals,<sup>3</sup> the use of waveguide structures with concentrated light beams along significant distances,<sup>4–6</sup> and other exciting developments, such as finding unexpected SHG in fibers and glasses.<sup>7</sup> Nevertheless, SHG is still limited because of the basic requirement for phase matching between the fundamental and the second-harmonic waves, which is usually not met due to dispersion. The most common method to overcome the phase-matching problem is to use the crystal birefringence. However, this and similar solutions restrict the frequency range in which the harmonic generation can be obtained. For example, the method cannot be used in  $\text{Sr}_x\text{Ba}_{1-x}\text{Nb}_2\text{O}_6$  (SBN) crystals in wavelengths below  $\sim 3 \mu\text{m}$  for  $x=0.75$  and  $\sim 2 \mu\text{m}$  for  $x=0.61$ , due to the relatively small birefringence of the crystal ( $\Delta n \approx 0.012$  for  $x=0.75$  and  $\Delta n \approx 0.029$  for  $x=0.61$  at wavelengths around  $0.83 \mu\text{m}$ ,<sup>8</sup> where the dispersion gives  $\Delta n \approx 0.2$ ). As far as we know, there is no reported experimental study of SHG with SBN. There is another way to obtain quasi-phase matching by an “artificial” spatial modulation of the optical nonlinearity (quasi-phase matching).<sup>2</sup> Such a modulation was produced in  $\text{LiNbO}_3$  and other crystals by a periodic changing of the crystal orientation during their growth,<sup>9</sup> or by other irreversible techniques.<sup>4–6</sup> This again gives SHG only for a specific input wavelength.

In this work we have demonstrated the following new points: (i) The first experimental use of SBN crystals for SHG. (ii) SHG for a broad range of input wavelengths (750–1064 nm) without any temperature or angular tuning of the crystal, by using a spread spectrum for phase matching. (iii) A novel fixing method, based on screening that produced ordered and random microferroelectric domain structures.

SBN is one of the most intensively studied photorefractive crystals due to its large electro-optic coefficient.<sup>10–12</sup> In

the photorefractive effect, an internal space-charge electric field is built in the crystal by light-induced charge separation. Large alternating internal fields on the order of kV/cm and periods between 0.1 and  $10 \mu\text{m}$  can be easily induced.<sup>12,13</sup> There are also ways to “fix” the electronic space-charge structure by inducing permanent ionic changes in the crystal.<sup>11,14</sup> The basic idea in this letter is to use controllable methods to induce a periodic domain structure in a photorefractive crystal, and to obtain the needed quasiphase matching for SHG. The fact that the required phase-matching period, which is on the order of a few  $\mu\text{m}$  (imposed by the dispersion), matches the optimal range for the photorefractively induced gratings in common crystals<sup>13</sup> is a very advantageous starting point. For that purpose, we have developed a new procedure for inducing a periodic and pseudorandom ferroelectric domain structure in photorefractive SBN crystals.

The experimental setup for the fixing process is shown in Fig. 1. Two mutually coherent beams derived from an argon ion laser with a wavelength of 514.5 nm and equal intensities (5–100 mW), formed an interference pattern in the crystal that is dependent on the angle between the beams. The crystals we used were poled  $\sim 5 \times 5 \times 5 \text{ mm}^3$  SBN with  $x=0.61$  and  $x=0.75$  and a nominal doping of 0.1 and 0.05 wt % Ce. The beams, of ordinary polarization, were focused into the crystal via a cylindrical lens ( $f=8 \text{ cm}$ ) giving an illuminated light layer in the crystal in the beams’ plane, which was perpendicular to the  $c$  axis (see Fig. 1). The layer had a thickness of  $\approx 30 \mu\text{m}$ . An

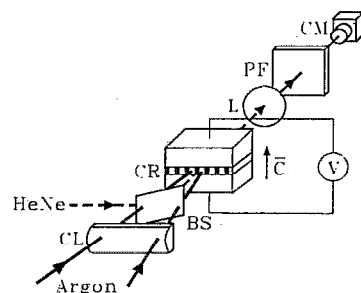


FIG. 1. The experimental setup for the fixing process. CR is the crystal with the indication of the  $c$  axis; CL is a cylindrical lens with a focal length of 8 cm; BS, L, PF, and CM are beamsplitter, lens, polarizer plus filter and camera for viewing the crystal with the HeNe beam.

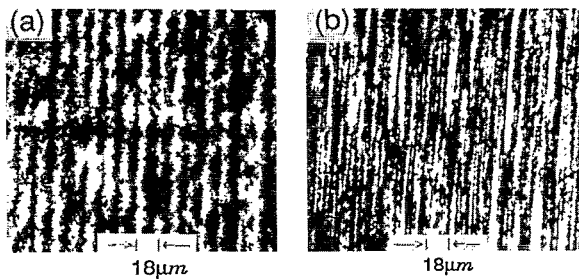


FIG. 2. Photograph of the crystal watched through a polarizer for (a) a fixed crystal viewed with an applied field of 500 V/cm. The interference pattern period of the argon beams used in this specific fixing process was  $\lambda_g = 18 \mu\text{m}$ , (b) microdomains in a fixed crystal.

external voltage was applied along the  $c$  axis with an opposite polarity to that used to pole the crystal. The voltage was gradually increased from 0 to 2 kV in 5 to 30 s. (The voltage corresponding to the coercive field is about 1.2 kV.) Then we blocked the beams and a voltage of about 1 kV was applied with a positive polarity (to that used for the poling). The fixing process was probed by a 1 mW HeNe laser beam with an input polarization at  $45^\circ$  with the  $c$  axis. In order to notice changes in the polarization due to the domains, the crystal was monitored through a polarizer with an axis perpendicular with respect to the input polarization.

We observed a domain structure in the crystal, as shown in Fig. 2(a). It was seen when an auxiliary voltage of 300 V was applied on the crystal. In some of the crystals it could be seen without this voltage. The horizontal dark line in the figure is the region of the argon ion light layer. The domain structure spread over most of the crystal's volume due to this seed layer. The spatial modulation was in the direction perpendicular to the  $c$  axis. The periodicity in Fig. 2(a) was  $18 \mu\text{m}$ . This periodicity, however, was controllable by changing the angle between the two argon ion laser beams which were used for the fixing. We were able to lower the periodicity down to  $\sim 1.5 \mu\text{m}$ . Successive domains were antiparallel ( $180^\circ$  type), evident from the fact that in the SHG experiment described below we could not see any significant conversion when the pump wave propagated along the  $c$  axis. SHG was observed for a light propagation along one of the other principle axes.

We believe that the fixing is based on screening. The applied field was screened in the regions with strong light intensities, by a separation of moving photoionized charges. The screening produced a distribution of the applied voltage which followed the light intensity pattern in the illuminated layer, causing a selective inversion of the spontaneous polarization. In fact, the domain structure started at the plane boundaries of the layer and then it spread over most of the crystal volume. At the end of the process the layer transformed into a visibly deformed layer, seen as a horizontal strip in Fig. 2(a). The light layer, of which width had to be limited to a few tens of  $\mu\text{m}$  (on the order of the domains' width), was important for the starting of the domain formation as it relaxed the constraint of the constant and uniform applied voltage on the crystal. (We can add that a thermal heating can also be a factor

that enhances the domain formation, especially in these crystals with a phase transition of  $50\text{--}80^\circ\text{C}$ , which are very close to room temperature.) Reference 11 reports on another method for modulating the spontaneous polarization of the crystal. A light fringe pattern with a modulation direction parallel to the  $c$  axis (compared to a perpendicular modulation in our case) caused an internal photorefractive field. An external voltage with a direction opposite to the crystal polarization, resulting in a field slightly smaller than the macroscopic coercive field, was applied on the crystal. The field caused a partial switching of the polarization in regions where the internal field was constructively added to the applied field. This seems to be a more straightforward method for obtaining uniform domain structures in the whole crystal volume. However, in this case the spontaneous polarization is modulated along the  $c$  axis, and a nonzero nonlinear coefficient with quasiphase matching is possible only for a beam propagation with an angular offset to the main crystal axes (adding the problems of beam walkoff).

In addition to the ordered domains we also observed pseudorandom domains in the same crystal, as shown in Fig. 2(b). These domains can be obtained even with one argon ion beam that produces the light layer in the crystal. We think that a nonuniform filamentation of the voltage drop in the layer due to fluctuations in the light intensity gave this nonuniform structure. The domains were elongated boxes with a two-dimensional modulation, having a spread range of widths, and an orientation along the  $c$  axis. The cross-section sizes were distributed around the order of a few  $\mu\text{m}$ . Reference 8 reports on  $\text{Ba}_2\text{NaNb}_5\text{O}_{15}$  (BNN) crystals with microdomains, obtained in the growing stage, while attempts to grow microdomains in SBN failed. Here we see that such microdomains can be produced, changed, and controlled in a grown SBN crystal. It was possible to erase the ordered domains and the microdomains by a gradual cooling of the crystal from above the paraferroelectric phase transition temperature, while applying an external field (5 kV/cm) and shining the crystal with a 100 mW argon ion laser beam to compensate the depolarization field by the excited carriers. In most cases the heating and cooling was unnecessary.

In the SHG experiment, the crystal was illuminated with a pulsed Ti-sapphire laser pumped by a  $Q$ -switched Nd:Yag laser (NY-61, Continuum Inc.). The pulses had a duration of 10 ns, a repetition rate of 10 Hz, and an average energy of about 40 mJ. However, most of our experimental data was taken with more moderate energies of 1–10 mJ. When the "treated" crystal was illuminated in the region with the fixing, a strong SHG was generated. The pump beam had an extraordinary or ordinary polarization and propagated in one of the two main axes which are perpendicular to the  $c$  axis (in parallel or in perpendicular to the direction of the ordered grating modulation). The SHG, however, always had an extraordinary polarization. It had a far-field spread in a direction perpendicular to the plane which contained the incident wave and the  $c$  axis (Fig. 3). The angular spread was about  $8^\circ$ . An angular spread was also reported for a BNN crystal with

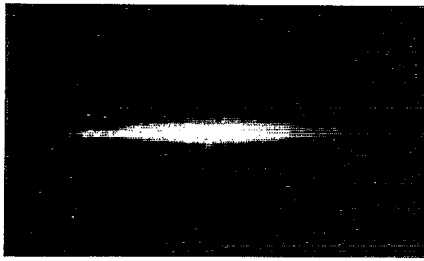


FIG. 3. Photograph of the far field of the harmonic wave. Here the wavelength of the harmonic wave was 435 nm.

grown microdomains. Here we were able to observe SHG for an input wavelength in the range between 750 and 910 nm with the Ti:sapphire laser and at 1064 nm with the pump Nd:Yag laser. Figure 4 shows the dependence of the conversion efficiency on the pump wavelength for the two cases of fixed crystals (random domains, with and without ordered domains). For input wavelengths below 800 nm, the second harmonic (400 nm) begins to lie inside the absorption band of the crystal and it is strongly attenuated. However, we presume that the technique allows obtaining SHG beyond the above range, especially for higher wavelengths, where attenuation is not a problem. The conversion efficiency ran around  $\approx 0.01\%$  for an unfocused input beam, having a peak power of about 0.5 MW and a beam diameter of 3 mm. However, with a slight focusing of the input beam into the crystal with an input of 2 MW we easily obtained conversion efficiencies of  $\approx 1\%$ . No change in the conversion efficiency was seen during 3 months. Without the fixing we did not see any significant SHG. This check was made in the crystal before the domain treatment, and also after the domains were erased.

The experimental results can give more information on the SHG process. The directions of the beams' propagation, polarizations, and the domains show that the significant nonlinear coefficients are  $d_{31}$  and  $d_{33}$ . By measuring the intensities of the harmonic waves we can estimate that  $d_{33} \sim 2d_{31}$ . This fits the theoretical estimation<sup>8,10</sup> for SBN with  $x=0.75$  that gives  $d_{33} = 12.8 \pm 3.6$  and  $d_{31} = 5.0 \pm 3.0$ ,

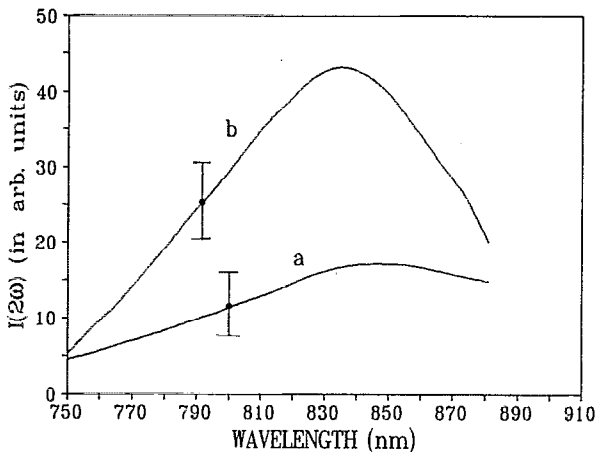


FIG. 4. Dependence of the conversion efficiencies on the pump wavelength for the crystal with microdomains only (curve a), and ordered plus microdomains (curve b).

in units which are relative to  $d_{36}$  of KDP. We believe that the domains make up for the phase mismatch between the fundamental and the second-harmonic waves,  $\delta k = k_{2\omega} - 2k_{\omega}$ , caused by an index difference (dispersion), which is  $\Delta n \approx 0.19$  for the 830 nm  $\rightarrow$  415 nm conversion region. This necessitates a domain grating period of  $\Lambda_g = 2\pi/\delta k = \lambda_0/2\Delta n \approx 2.07 \mu\text{m}$ , where  $\lambda_0$  is the vacuum input wavelength. However, for our results with the broadband spectral response shown in Fig. 4, we must have had spread quasiphase matching means. Such a mechanism was theoretically discussed in the past.<sup>15</sup> In our experiment this is provided by the random microdomains in the crystals. Their net effect is shown in curve (a) of Fig. 4, taken with the crystal that had only the microdomains. The ordered domains, with the well-defined periodicity along the beam propagation direction, are responsible for the selective enhancement of a narrow spectral regime, as shown in curve (b). They also gave the enhanced peaks in the spread far field (not observed in Fig. 3). The periodicity, which in this experiment was  $\approx 2 \mu\text{m}$  fits the enhanced response. It was also possible to obtain a very narrow spectral range of  $\sim 0.5$  nm, of which center was controllable by the grating wavelength. Then the SHG was a narrow beam. Another important advantage of the spread phase matching is that it relaxes the usual strict demand for a precise direction and optimum shape of the pump beam in SHG. There is, of course, a price for all these advantages, paid by a degradation of the efficiency.<sup>15</sup>

In conclusion, we point out several potential uses of this work. First of all, we can have a simple means for a coherent light source in the 380–500 nm wavelength range with the Ti:sapphire laser. This range also fits GaAs semiconductor lasers. It can be also used in the standard SHG technique for short pulse inspection of the important mode-locked Ti:sapphire lasers. Finally, we note that similar techniques might be applied for the use of other crystals (bulks or fibers) for SHG in a prespecified spectral range.

<sup>1</sup>P. Franken, A. E. Hill, C. W. Peters, and G. Weinreich, Phys. Rev. Lett. 7, 118 (1961).

<sup>2</sup>N. Bloembergen, *Nonlinear Optics* (Benjamin, London, 1982).

<sup>3</sup>*Nonlinear Optical Properties of Organic Molecules and Crystals*, edited by D. S. Chemla and J. Zyss (Academic, New York, 1987); D. Josse, S. X. Dou, J. Zyss, P. Andereazza, and A. Perigaud, Appl. Phys. Lett. 61, 121 (1992).

<sup>4</sup>M. L. Bortz and M. M. Fejer, Opt. Lett. 17, 704 (1992).

<sup>5</sup>K. Yamamoto, K. Mizuuchi, and T. Taniuchi, Opt. Lett. 16, 1156 (1991).

<sup>6</sup>K. Shinozaki, Y. Miyamoto, H. Okayama, K. Kamijoh, and T. Nonaka, Appl. Phys. Lett. 58, 1934 (1991).

<sup>7</sup>U. Osterberg and W. Margulis, Opt. Lett. 12, 57 (1987).

<sup>8</sup>A. M. Prokhorov and Y. S. Kuzminov, *Ferroelectric Crystals for Laser Radiation Control* (Higler, England, 1990); A. L. Aleksandrovskii and A. I. Nagaev, Solid Status Solidi A 78, 431 (1978); A. L. Aleksandrovskii, Vestnik Mosk. Univers.: Ser. Phys. Astron. 22, 51 (1981).

<sup>9</sup>A. Feisst and P. Koidl, Appl. Phys. Lett. 47, 1125 (1985).

<sup>10</sup>C. R. Jeggo and G. D. Boyd, J. Appl. Phys. 41, 2741 (1970).

<sup>11</sup>F. Micheron, C. Mayeux, and J.C. Trotier, Appl. Opt. 13, 784 (1974).

<sup>12</sup>B. Fischer, M. Cronin-Golomb, J. O. White, A. Yariv, and R. Neurgaonkar, Appl. Phys. Lett. 40, 863 (1982).

<sup>13</sup>G. Valley and M. B. Klein, Opt. Eng. 22, 704 (1983).

<sup>14</sup>J. P. Herriau and J. P. Huignard, Appl. Phys. Lett. 49, 1140 (1986).

<sup>15</sup>M. Nazarathy and D. W. Dolfi, Opt. Lett. 12, 823 (1987).